THE EFFICIENCY OF HYDRAZINE-PEROXIDE FUEL CELLS

H. B. Urbach and R. J. Bowen

Naval Ship Research and Development Laboratory
Annapolis, Maryland

INTRODUCTION

Hydrazine fuel cells may be a contender in some future applications of fuel-cell power (reference 1). However, the precise evaluation of the hydrazine fuel cell relative to other cells requires a knowledge of their realizable experimental coulombic efficiencies. The inefficiencies characteristic of hydrazine fuel cells are caused largely by self decomposition of the hydrazine, cross diffusion of hydrazine and oxygen through the porous structure of the cell, and by bleed of oxygen from the cell. A sample evaluation of such coulombic inefficiencies is made in this report based upon laboratory analysis of a single 6-in by 6-in cell employing platinum catalyzed fuel cells. The revelancy of the data is quite general. However, the specific assignment of numerical values of efficiency to other systems should only be employed with the knowledge that considerable variation exists not only between different commercial systems but within individual systems.

DESCRIPTION OF THE EQUIPMENT

Mechanical Features of the Experimental Apparatus

High ambient pressures were developed in a pressurized system

similar to that shown in Figure 1. The pressure chambers were 5-in and 9-in diameter steel vessels rated at 15,000 and 30,000 psi respectively. Pressurization of the system was achieved with high pressure argon and oxygen compressed with air-driven compressors. Cells of 15 cm^2 (circular) and 232 cm^2 (6-in by 6-in square) were employed. The hydrazine-electrolyte mixture was circulated past the anode with a magnetically coupled centrifugal impeller for the small cell with a pressure-equilibrated submersible centrifugal pump in the large cell. The electrolyte flow was monitored with a turbine flow meter (FI).

Electronic Components of the Experimental Apparatus

Polarization data were obtained by programming the current sweep of a 50-amp Kordesch-Marko-type current interrupter and gate (reference 2), recording sequentially by means of a stepping switch, the anode, cathode and cell potential (including cell potential corrected for ohmic losses).

Fuel Cell Components

The anodes were commercially supplied pressed teflon-platinum

powders on gold-plated nickel screens with platinum loadings of 9 mg/cm^2. The cathodes were the same except that the platinum loadings were 40 mg/cm^2. The electrolyte was fixed in a .030-in asbestos matrix. The electrolyte contained in the asbestos was in contact with the hydrazine-electrolyte mixture circulated behind the anode through the pores of the electrode. These pores permitted convection and/or diffusion of oxygen and nitrogen depending upon the differential pressure (indicated by the differential pressure gage DF in Figure 1) maintained between anolyte and catholyte compartments by the differential pressure regulator within the pressure vessel.

EXPERIMENTAL RESULTS

The major sources of the inefficiencies in the hydrazine-oxygen fuel cell are derived from self-decomposition of the fuel, cross diffusion of the oxidant and fuel, and from bleed of the oxidant. The experimental data on self-decomposition are indicated in Figure 2. The arrows indicate the rate of gas evolution during increasing or decreasing load. Gas evolution rates include both hydrogen and nitrogen evolution. The dashed line increasing with load represents only the theoretical nitrogen evolution discussed below. The ascending solid line is the straight line parallel to the theoretical line of nitrogen evolution which best approximates the experimental points. The descending solid line has the same absolute value of slope. The points show a fall-off in gas evolution which approaches a minimum at approximately 128 ml/min-ft^2 almost 67% of the open circuit approximation of 200 ml/min-ft^2.

Figure 3 represents the cross diffusion of hydrazine from the anolyte through the anode and cell matrix to the cathode where the hydrazine is oxidized to water and nitrogen. The cross diffusion is measured by analysis of the evolved gases rather than by electrochemical analyses as in reference 1. The diffusion is dependent upon the applied load as well as the hydrazine concentration. The equivalent hydrazine loss is given in ml/min-ft^2 for water-saturated nitrogen at 25° C and in equivalent amp/ft^2. Gas volumes are always water-saturated at 25° C in all graphs and tables.

The most significant fact relative to efficiency is that the cross diffusion losses of hydrazine decrease rapidly with load. At low concentrations of hydrazine the ratio of cross-diffusion losses at open circuit and at load is much higher than the ratio at high concentrations of hydrazine. For example, at 1% hydrazine the ratio is approximately 20 whereas at 3% the ratio is approximately 4.5.

Table I contains the raw data used to calculate efficiency in subsequent figures. Figure 4 illustrates the effect of experimental bleed rates on the cell potential at various loads. The cell potential is logarithmically dependent upon the bleed rate within the experimental limits of study. However, the logarithmic dependence is not uniform with current density, exhibiting increasing slope with the load. Thus bleeds rates effect increased cell output most strongly at high loads.

DISCUSSION

Self-Decomposition Losses

Experimental gas-evolution data for hydrazine decomposition have

been reported in the open literature (reference 2). It is possible to rationalize the shape of the experimental curves. If it is assumed that the mechanism of self-decomposition of hydrazine proceeds according to the following half cell and overall reactions:

$$N_2H_4 + 4OH^- \longrightarrow N_2 + 4H_2O + 4e \qquad (1)$$

$$4H_2O + 4e \longrightarrow 2H_2 + 4OH^- \qquad (2)$$

$$N_2H_4 \longrightarrow 2H_2 + N_2 \qquad (3)$$

then as the potential of the electrode becomes more anodic, reaction (2) will be suppressed while reaction (1) is accellerated. For every four equivalents of charge one mole of nitrogen will be produced and 2 moles of hydrogen will be consumed. Thus:

$$V_n = V_n^o + \frac{K I}{4} \qquad (4)$$

$$V_h = V_h^o - \frac{K I}{2} \qquad \text{for } I \leq 2V_h^o / K \qquad (5)$$

where V_n and V_h are the volumes in liters of nitrogen and hydrogen produced per min-ft^2, V_n^o and V_h^o are the volumes produced under open circuit conditions, K is (298/273) (22.4 x 60)/96,500 and I is the current density in amp/ft^2. When the current density exceeds $2V_h^o / K$, V_h vanishes. The total gas production rate, V_t, is given by the sum of Equations (4) and (5). Recognizing from Equation (3) that $2V_n^o$ equal V_h^o we obtain:

$$V_t = 3V_n^o - \frac{K I}{4} \qquad \text{for } I \leq 2V_h^o / K \qquad (6a)$$

$$V_t = V_n^o + \frac{K I}{4} \qquad \text{for } I \geq 2V_h^o / K \qquad (6b)$$

Thus, the slope of the descending portion of the gas evolution curve at

low current densities is equal in absolute value to the slope of the ascending curve. The minimum occurs when the two branches of the curves in Equations (6) are equal whence, at the minimum,

$$I_{min} = 4V_n^o / K \qquad (7)$$

and

$$V_{t_{min}} = 2V_n^o \qquad (8)$$

Thus at the minimum, the total volume of gas should correspond to 67% of the open circuit gas evolution. Furthermore, the slopes of the ascending branch of the curve should be KI/4, in agreement with the theoretical value indicated by the dashed curve. These conclusions are closely approximated in Figure 2 and in the results of reference 2.

There is one area of divergence between theory and results. In previous studies (unpublished) analytical data on gas evolution indicate that not all of the hydrogen is consumed. This result would suggest that some self-decomposition does not occur at the electrodes but on insulated metallic or catalytic surfaces which cannot accomodate electrochemical discharge of the evolved hydrogen.

Thus the current of minimum gas evolution at approximately 15.5 amp/ft^2 in Figure 2 might normally be expected to correspond with the current of self-decomposition indicated by the back-extrapolated (to zero) ascending branch of the curve which indicates 20 amp/ft^2. The difference, 4.5 amp/ft^2 (corresponding to 1.5 amp/ft^2 since only a third of this gas should be nitrogen) might reasonably be interpreted as self-decomposition

on insulated metal surfaces.

Cross Diffusion Losses

The results of Figure 3 may be compared with previous studies of cross diffusion reported in reference 1. The data of reference 1 were obtained by a potentiostatic analysis of hydrazine under open circuit conditions. The present data, interpolated to 30° yield a cross-diffusion loss of approximately 9.5 amp/ft^2 in good agreement with the value of 8 amp/ft^2 obtained from Figure 3 (at 3% hydrazine) considering the differences in the experimental conditions.

The significant features of the data in Figure 3, namely that losses arising from cross diffusion decrease with load, arise from the fact that under load the available hydrazine is more rapidly consumed. Most interesting is the fact that the cross-diffusion loss at lower concentrations of hydrazine is significantly less than half the loss at higher concentrations. In particular, for example, at the 80-amp load, the loss at 2% hydrazine is only 35% of the loss at 3%.

The possibility that cross diffusion of oxygen decreases with load is suggested by these results.

Bleed Losses

The data of Figure 4 represent not only bleed losses, but cross diffusion of hydrazine. The nitrogen which is observed in the oxygen bleed was originally part of the hydrazine which was transported by diffusion from the anolyte flowing past the backside of the anode through the asbestos separator. Convection plays no role in the transport of this

hydrazine because the pressure gradient in the cell is normally against the direction of hydrazine flow.

The logarithmic dependence of the cell potential on oxygen bleed rate suggests that the cathode potential is exhibiting a Nernst-like response to the oxygen concentration which therefore should be linearly related to the bleed rate. While logarithmic proportionality may exist the slopes of the curves do not correspond to expected values for typical Nernst behavior. In addition, the slopes change with current density indicating more complex relationships.

Hydrazine Fuel Requirements

A formulation of fuel requirements is simply stated if it is assumed that there are only four significant elements of fuel-cell inefficiency, the diffusion of hydrazine to the cathode, D_n, the diffusion of oxygen to the anode, D_o, the bleed of oxygen from the cathode space, B, and the self decomposition of hydrazine, S. The weight per kw-hr of hydrazine, W_n, in terms of the weight per kamp-hr, M_n (0.663 lb/kamp-hr for pure hydrazine) is

$$W_n = \frac{M_n}{E}\left(\frac{I + D_n + D_o + S}{I}\right) \qquad (9)$$

where E is the cell output potential. The oxygen bleed term does not enter into the expression for fuel requirements.

In Table I the compilation of raw laboratory data, losses have been expressed in amp/ft^2 for consistency. The loss due to diffusion of oxygen, D_o, (see column 3 which contains the sum of D_o and

S) is obtained from Figure 5 which is reproduced from reference 1. The value of D_o is 1 amp/ft^2 corresponding approximately to the cross diffusion of 4500 psi and 50° C. The value of the self decomposition term, S, is 1.5 amp/ft^2 and is derived from Figure 2 in accordance with the discussion above. The average values for the cross diffusion of hydrazine, D_n, namely, 5.75, 3.7 and 3.8 amp/ft^2 were obtained experimentally and deviate from the values 7.8, 5.5 and 2.6 interpolated from Figure 3 and corrected for temperature. The results of Figure 3 represent a separate independent study at 30° C. The disparities result from aging processes and from difficulties associated with maintaining constant oxygen bleed, hydrazine diffusion rates, and differential pressures in a dynamic system. The results of Figure 3 exhibit a larger fall-off in the cross-diffusion rate as load increases than is apparent from column 2 of Table I. In fact according to Table I, the average cross diffusion, D_n, is slightly higher at 80 amp/ft^2 than at 40 amp/ft^2. Figure 3 indicates that such behavior is anomalous. The data of Table I represent measurements over a period of several hours in contrast with the data of Figure 3. Thus, they may represent changes in the differential pressure between anode and cathode spaces which modify the diffusion processes by superposition of convective flow patterns.

In the following analysis, the values of hydrazine diffusion, D_n, employed in subsequent calculations are those listed in Table I. The inconsistency described in the previous paragraph color the results of

the following analyses to the extent of +4% to -2% in the most discrepant cases. The discrepancy is on the conservative side in the most likely operating ranges.

Columns 6 and 7, the hydrazine fuel requirement calculated by use of Equation 9 are plotted as a function of the bleed rates in column 8 in Figure 6. The immediate conclusion to be drawn is that the oxygen bleed rate within the range of 1 to 5 amp/ft^2 does not change the fuel requirement by more than 1.5% and is therefore not the most significant factor in hydrazine fuel requirements.

Peroxide Requirements

A formulation of peroxide requirements is given in Equation 10. The weight per kw-hr of peroxide, W_o, in terms of the weight of peroxide required per kamp-hr, M_o, (1.398 lb/kamp-hr for 100% peroxide) is

$$W_o = \frac{M_o}{E} \left(\frac{I + D_o + D_n + B}{I} \right) \qquad (10)$$

The self-decomposition term, S, in Equation (9) is replaced by the bleed rate, B, in Equation (10). The value of D_o has again been arbitrarily set at 1 amp/ft^2 corresponding to the cross diffusion at 4500 psi and 50^o C. The values of D_n and B are taken directly from the measured raw data of Figure 4. See Table II for a compilation of the input raw data and calculated values of weights per kw-hr. The required weights are plotted against bleed rate in Figure 7. The significant fact again is that at current densities where operation is likely because of high efficiency, the bleed rate is essentially negligible in effect between 1 and 4 amp/ft^2.

Fuel-Oxidant Requirements

Figure 8 indicates that fuel-oxidant requirements per kw-hr (derived from Figures 6 and 7) exhibit broad minima with respect to oxygen bleed rate. The significant conclusion, as before, is that the oxygen bleed rate is **not** a significant factor at operating current densities such as 40 amp/ft^2 or greater which would be desirable for reasonable coulombic efficiency.

Figure 9 represents the specific fuel-oxidant requirements per kw-hr under varying load as determined by Figure 8. The effect of bleed rate is again seen to be small compared to the effect of load. In contrast with behavior observed in hydrogen-oxygen fuel cells, the specific fuel-oxidant requirements decrease with load until approximately 80 amp/ft^2. Increase in specific fuel-oxidant requirements probably increases above 80 amp/ft^2 where life characteristics of hydrazine fuel cells represent an uncertain area. Assuming acceptable life characteristics, maximum energy density appears to occur between 60 and 90 amp/ft^2. However, at least up to 80 amp/ft^2, the specific energy density of the tested cells does not exhibit a maximum when trade-off analyses are made involving the operating power of fuel cells and the power efficiency of fuel and oxidant.

Coulombic Efficiencies

Figures 10 shows that the coulombic efficiency of the peroxide (oxygen) cathode is a function of bleed rate exhibiting a maximum for high current densities in the neighborhood of 1 amp/ft^2. On the other hand, Figure 11

shows that the coulombic efficiency of the hydrazine anode is essentially independent of oxygen bleed rate over the range studied. Figures 12 and 13 show again that load rather than bleed is the significant overall factor in coulombic efficiency as in specific energy requirements.

SUMMARY

The coulombic efficiency and specific material requirements per energy unit of a hydrazine-peroxide single cell was studied. Electrodes were a commercially supplied variety prepared from pressed powdered platinum and teflon powders in 6-in. by 6-in. squares. Analysis of the gas evolution at hydrazine anodes indicates that at high loadings the self-decomposition losses of hydrazine may be negligible. Cross diffusion of hydrazine (and possibly oxygen) decrease rapidly with load. Bleed rates effect increases in cell potential most strongly at high loadings.

Hydrazine requirements decrease only slightly with bleed rate. On the other hand, peroxide requirements increase with bleed rate although at high loads the increase is small. Combined fuel-oxidant requirements per energy unit show broad minima with respect to bleed rate. At high current densities the fuel-oxidant requirements are essentially independent of bleed rate. However, they are strongly dependent upon load. Maximum energy density and coulombic efficiency may occur between 60 and 90 amp/ft^2.

The results are peculiar to the particular system studied. In any

systems analysis, numerical assignment of efficiencies should be based upon experimental evaluation of the fuel cell modules actually contemplated for application.

As a result of the increase of coulombic efficiency with load at least up to 80 amp/ft^2 no maximum may be expected when trade-off analyses are made involving the operating power density of fuel cells and the coulombic efficiency of fuel and oxidant consumption.

ACKNOWLEDGEMENTS

This work is part of a program of research sponsored by the Naval Ship Systems Command under the cognizance of Bernard Rosenbaum. The authors are pleased to acknowledge encouragement and discussion with John H. Harrison, Head of the Fuel Cell Branch of the U. S. Naval Ship Research and Development Laboratory, Annapolis.

GLOSSARY OF SYMBOLS

B = Bleed loss of oxygen in amperes per square foot

D_n = Diffusion loss of hydrazine in amperes per square foot

D_o = Diffusion loss of oxygen in amperes per square foot

E = Cell potential in volts

I = Current density in amperes per square foot

K = A constant

M = Mass requirements per kiloampere-hour

M_n = Wt of hydrazine-water mix per kiloampere hour

M_o = Wt of peroxide-water mix per kilowatt hour

S = Self-decomposition loss of hydrazine

V_h = Volume of hydrogen in liters produced per minute per square foot

V_n = Volume of nitrogen in liters produced per minute per square foot

V_t = Volume of all gases in liters produced per minute per square foot

W_n = Wt of hydrazine-water mix per kilowatt hour

W_o = Wt of peroxide-water mix per kilowatt hour

REFERENCES

1. R. J. Bowen, H. B. Urbach, D. E. Icenhower, D. R. Gormley and R. E. Smith, "The Hydrazine-Oxygen Fuel Cell at Ambient Deep Sea Pressures", NSRDC Report 2671, February 1969. Published for the Intersociety Energy Conversion Engineering Conference in "IECEC '68 Record" by the Institute of Electrical and Electronics Engineers, Inc., New York, 1968.

2. V. S. Daniel'-Bek and G. V. Vivitskaya, Elektrokhimiya, 3, 8 (1967).

TABLE I - FUEL REQUIREMENTS

I Amp/ft^2	D_n Amp/ft^2	$D_o + S$ Amp/ft^2	$\frac{I + D_n + D_o + S}{I}$	E Volt	Wt (100%) (.663) lbs/kw-hr	Wt(90%) lbs/kw-hr	B Amp/ft^2	Coulombic Efficiency
20	5.7	2.5	1.410	.895	1.045	1.161	.3	.7092
20	5.8	2.5	1.415	.899	1.004	1.159	.9	.707
20	5.8	2.5	1.415	.907	1.034	1.149	1.8	.707
20	5.7	2.5	1.410	.907	1.031	1.146	2.8	.7092
20	5.7	2.5	1.41	.910	1.027	1.141	5.5	.709
40	3.5	2.5	1.15	.849	.898	.998	.3	.870
40	3.5	2.5	1.15	.858	.889	.988	.8	.870
40	3.7	2.5	1.155	.865	.885	.984	1.6	.8658
40	3.5	2.5	1.15	.864	.882	.980	2.1	.870
40	3.5	2.5	1.15	.869	.877	.974	4.5	.870
80	3.8	2.5	1.079	.838	.854	.949	1.1	.927
80	3.4	2.5	1.074	.846	.842	.935	2.7	.931
80	4.2	2.5	1.084	.849	.846	.940	2.9	.923

TABLE II - PEROXIDE REQUIREMENTS

I	D_{n+B}	$\frac{I + D_o^* + D_{n+B}}{I}$	E	$\frac{(1.398)}{\text{Wt/kw-hr}}$ 100%	Wt/kw-hr	B	Coulombic Efficiency
20	6	1.35	.895	2.109	2.343	.3	.741
20	6.7	1.385	.899	2.158	2.393	.9	.722
20	7.6	1.43	.907	2.204	2.45	1.8	.699
20	8.5	1.475	.907	2.273	2.526	2.8	.678
20	11.2	1.61	.910	2.473	2.748	5.5	.621
40	3.8	1.12	.849	1.844	2.05	.3	.893
40	4.3	1.13	.858	1.841	2.046	.8	.885
40	5.3	1.156	.865	1.868	2.076	1.6	.865
40	5.6	1.165	.864	1.885	2.094	2.1	.858
40	8.0	1.225	.869	1.971	2.190	4.5	.816
80	4.9	1.074	.838	1.792	1.991	1.1	.931
80	6.1	1.089	.846	1.80	2.00	2.7	.918
80	7.1	1.101	.849	1.813	2.014	2.9	.908

* D_o is chosen as the value at 50°C and 4500 psi, namely 1. amp/ft^2.

TABLE III - FUEL-OXIDANT REQUIREMENTS

I Amp/ft^2	Fuel Wt per kw-hr	Oxidant Wt per kw-hr	Total Wt per kw-hr (100%)	Total Wt per kw-hr (90%)	B
20	1.045	2.109	3.154	3.504	0.3
20	1.044	2.158	3.202	3.558	0.9
20	1.034	2.204	3.238	3.598	1.8
20	1.031	2.273	3.304	3.671	2.8
20	1.027	2.473	3.50	3.889	5.5
40	.898	1.844	2.742	3.047	0.3
40	.889	1.841	2.73	3.033	0.8
40	.885	1.868	2.753	3.059	1.6
40	.882	1.885	2.767	3.074	2.1
40	.877	1.971	2.848	3.164	4.5
80	.854	1.792	2.646	2.94	1.1
80	.842	1.80	2.642	2.936	2.7
80	.846	1.813	2.659	2.954	2.9

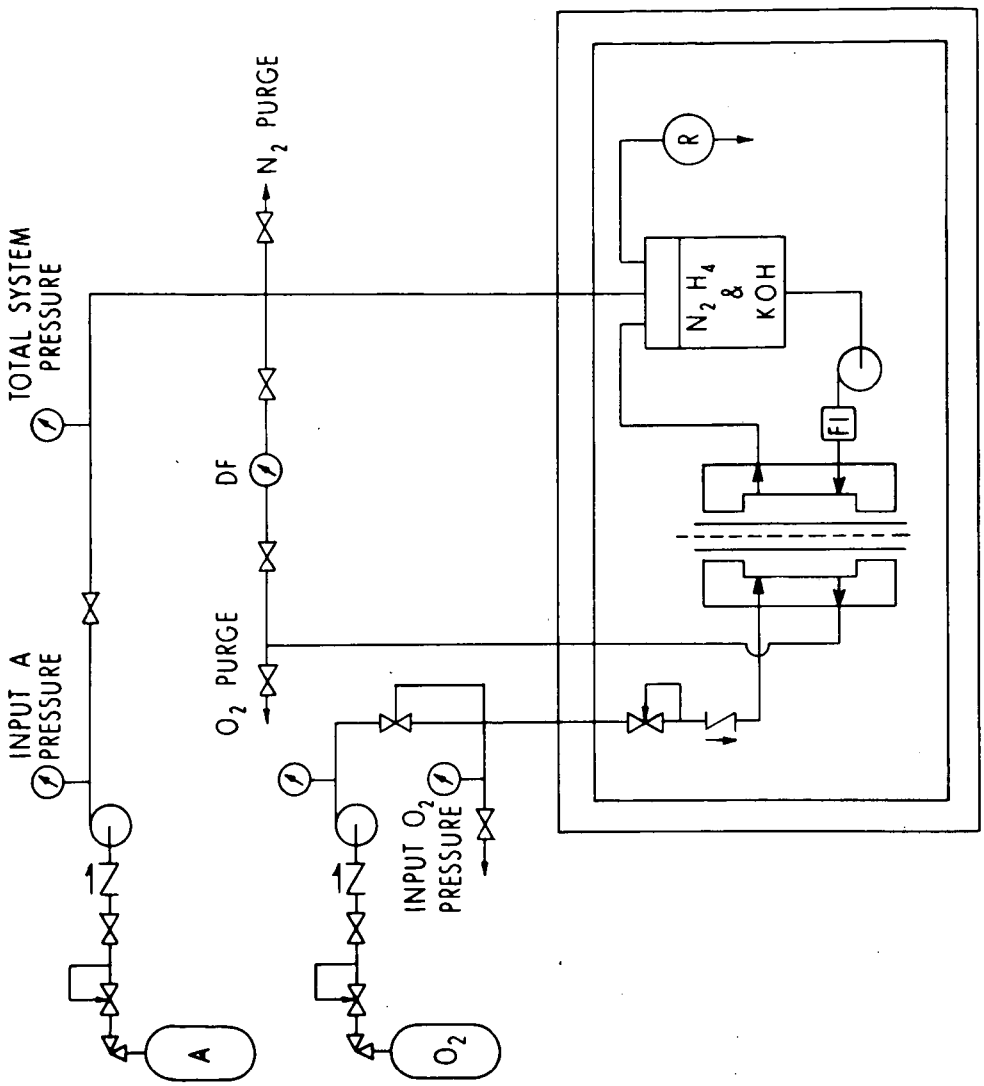

Figure 1 - Experimental apparatus for studying fuel cells under pressure.

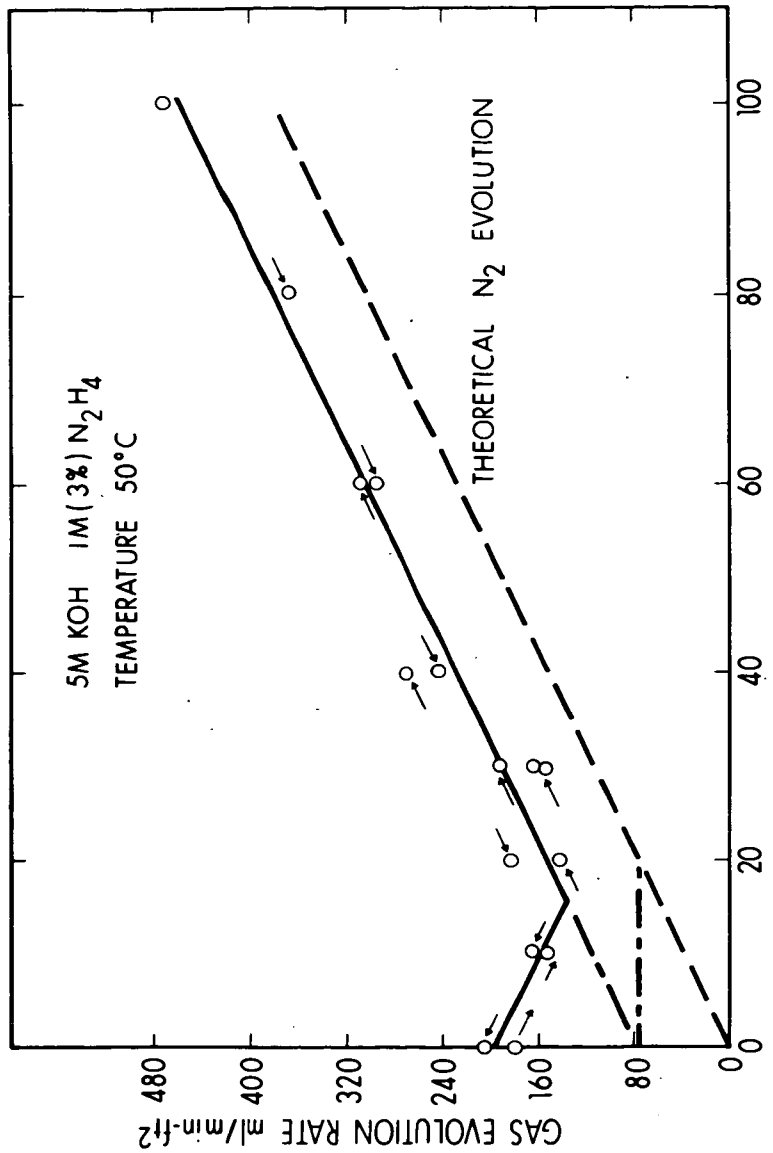

Figure 2 - Gas evolution at platinum-teflon anodes (platinum loading is 9 mg/cm^2) exposed to hydrazine.

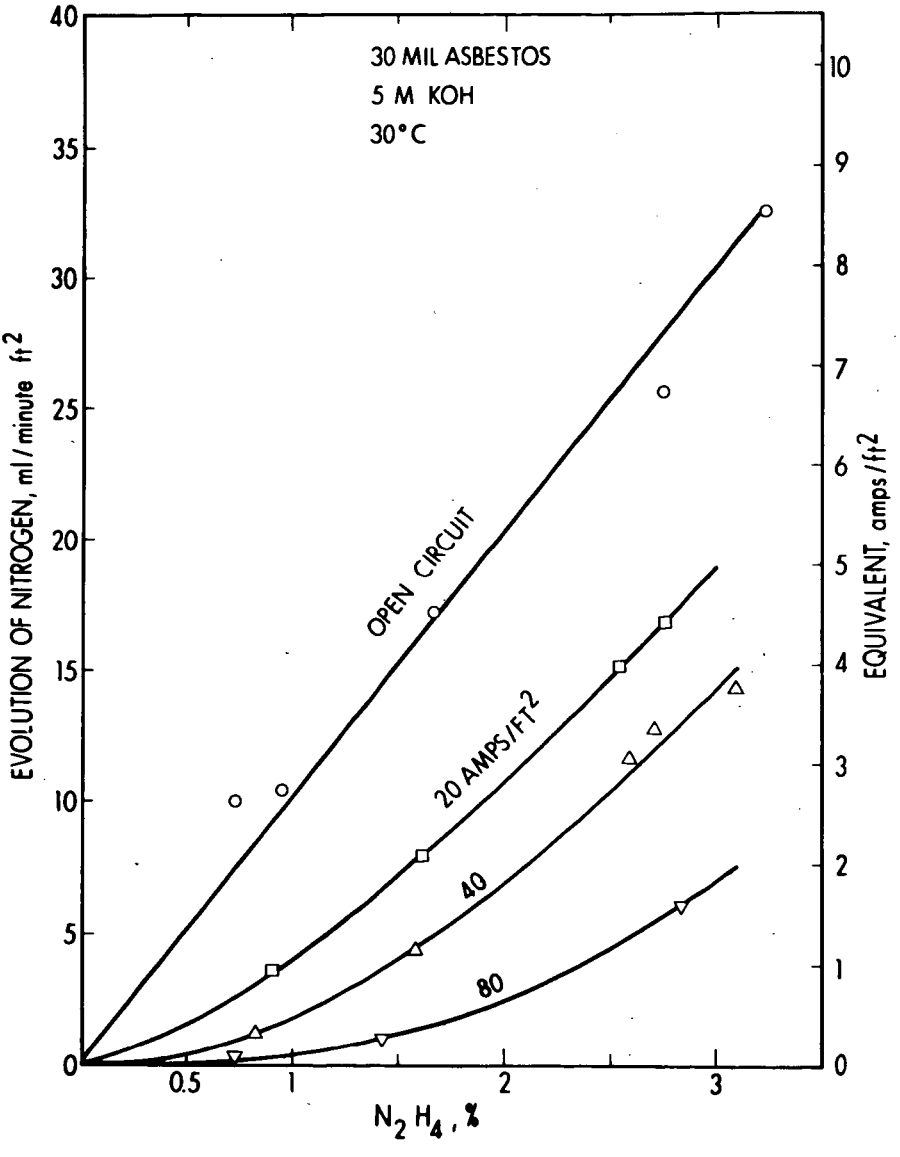

Figure 3 - Effect of hydrazine concentration and load on nitrogen evolution at a platinum anode.

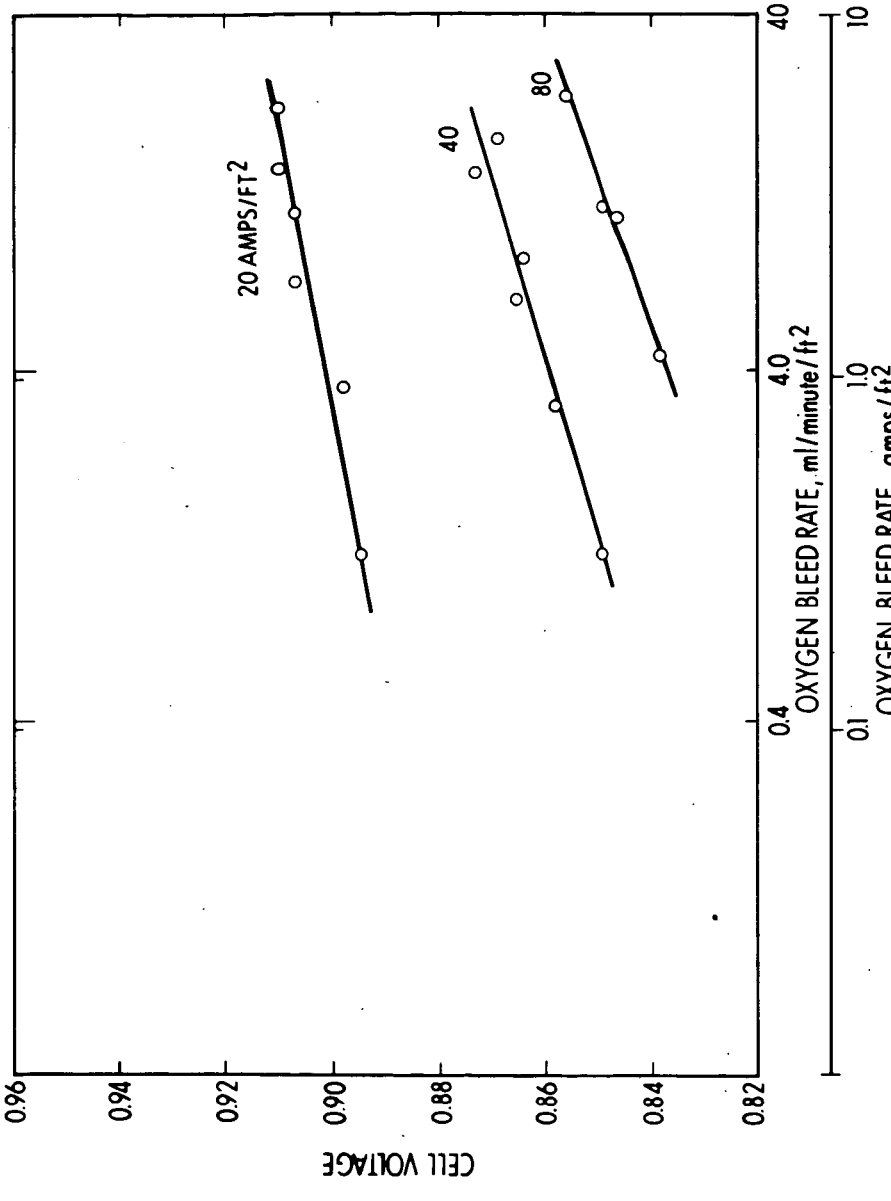

Figure 4 - Effect of load and oxygen bleed rate on the output potential of a hydrazine-oxygen cell.

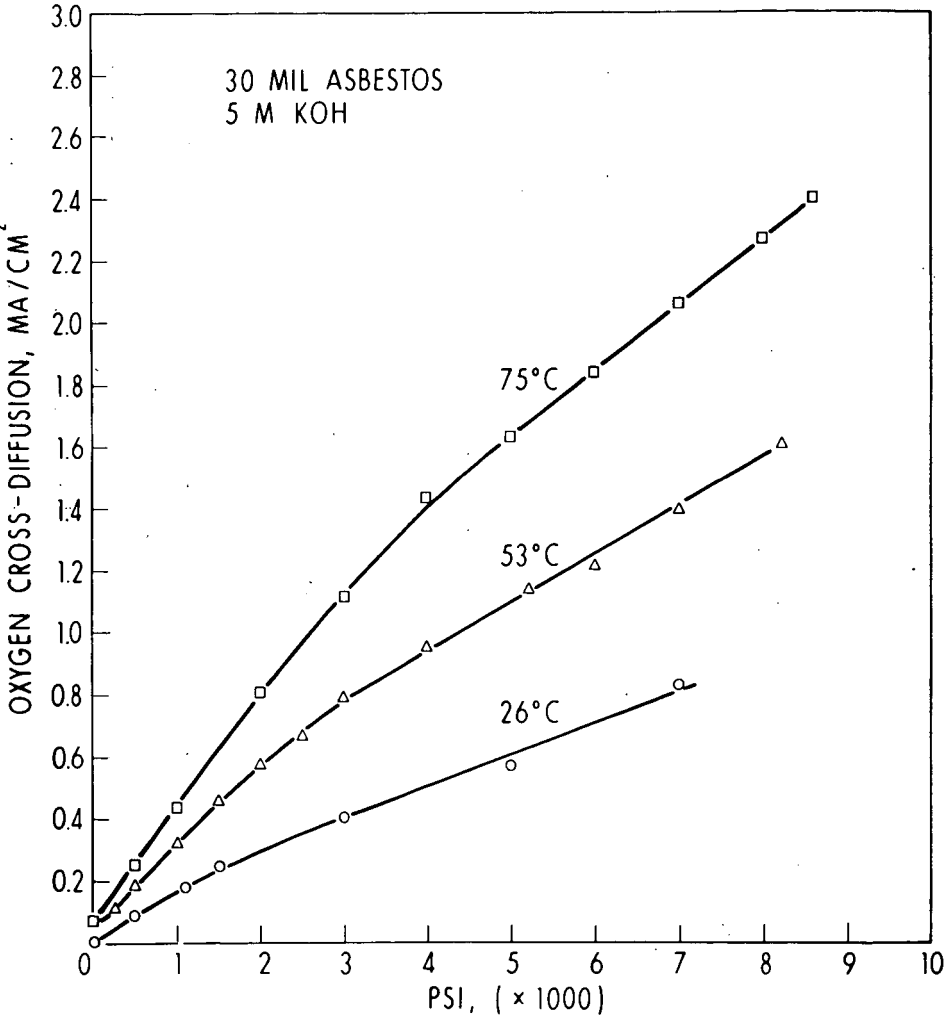

Figure 5 - Effect of pressure on the cross diffusion of oxygen through an asbestos separator in a hydrazine-oxygen cell.

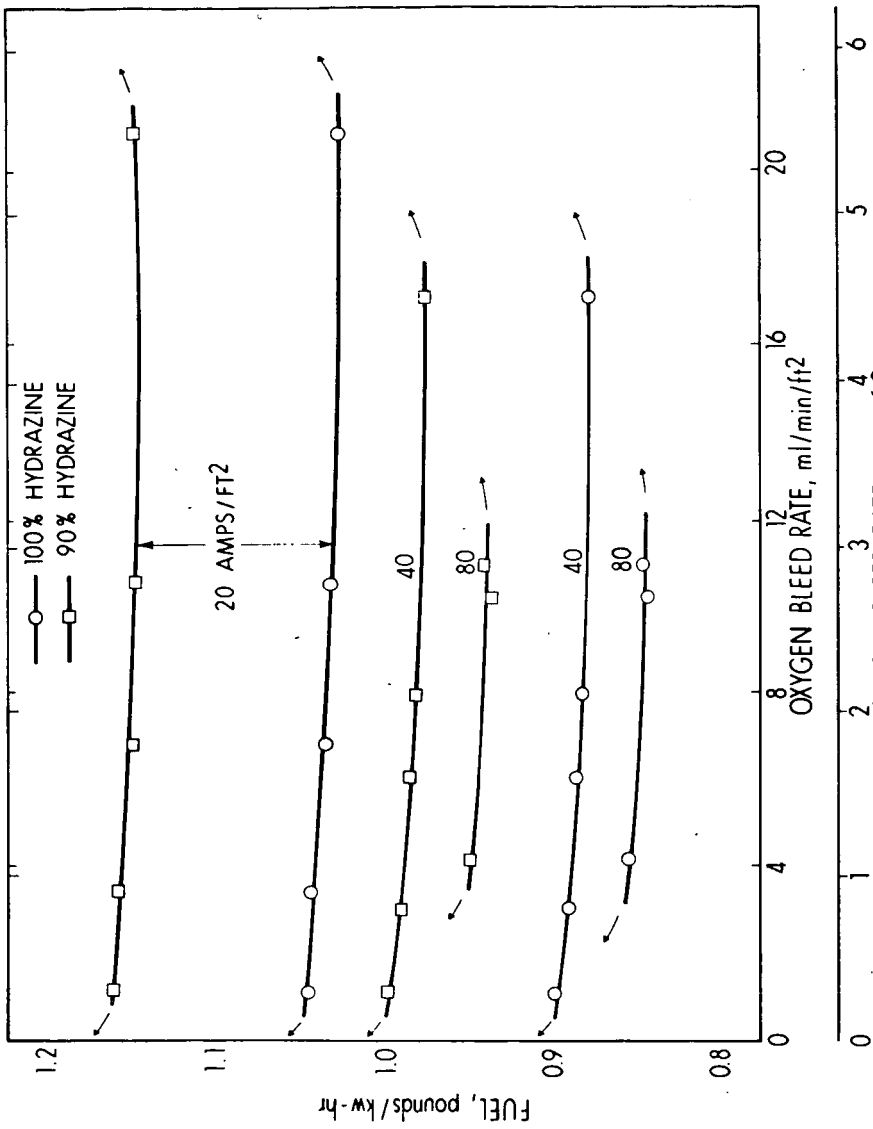

Figure 6 - Effect of oxygen bleed rate on the hydrazine fuel requirements per kw-hr.

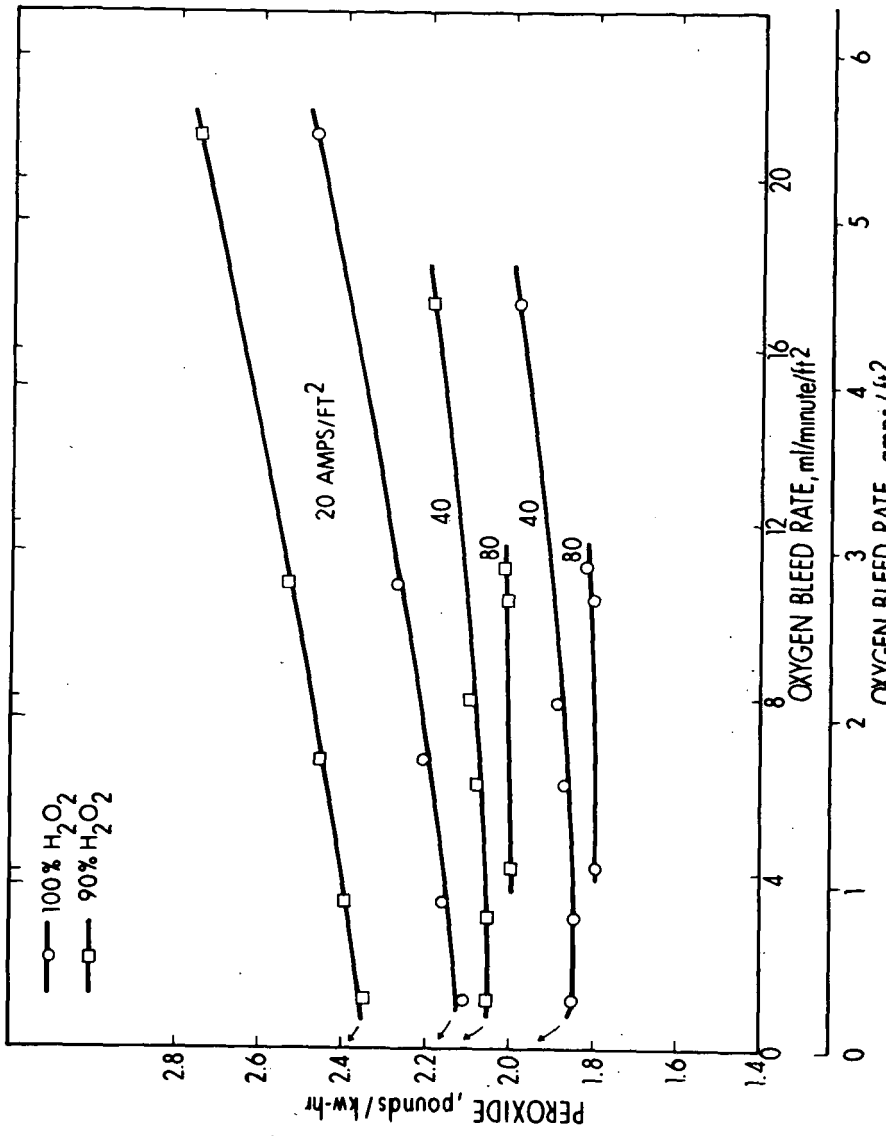

Figure 7 - Effect of oxygen bleed rate on peroxide requirements per kw-hr.

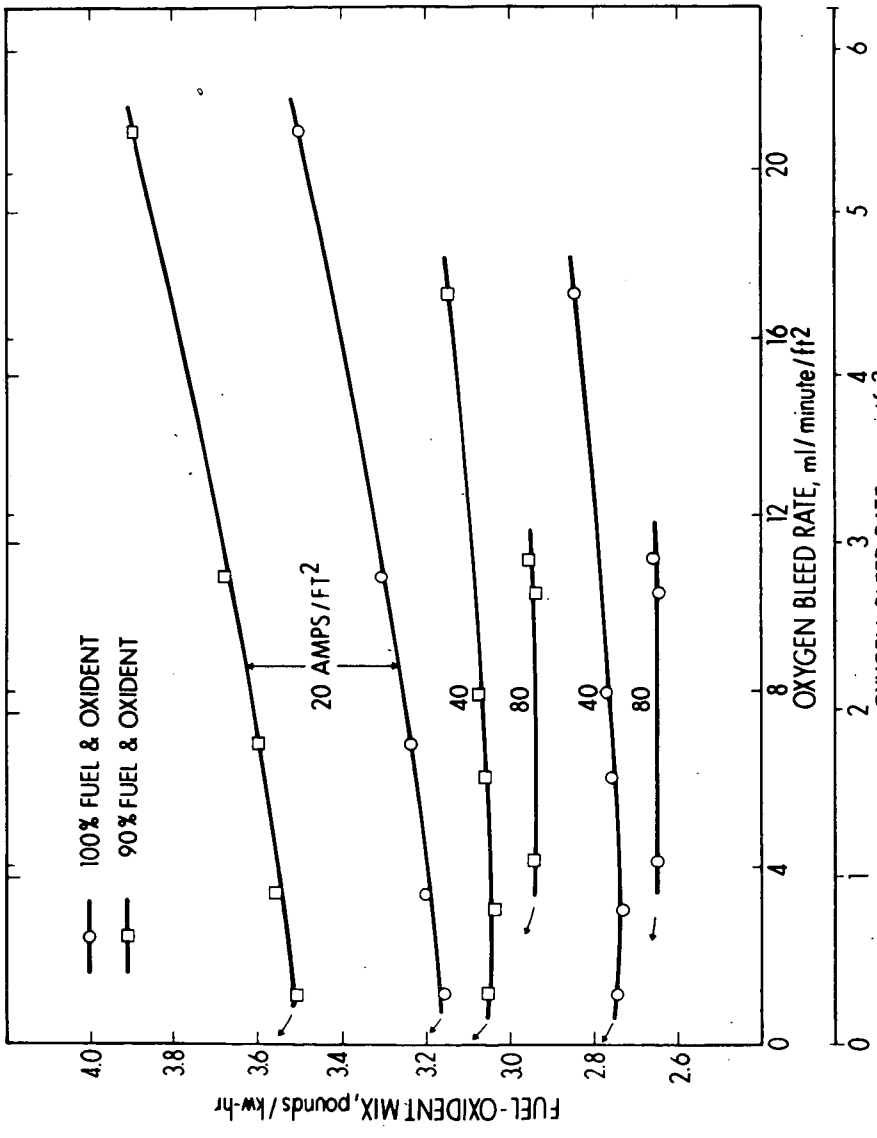

Figure 8 - Effect of oxygen bleed rate on hydrazine-peroxide requirements per kw-hr.

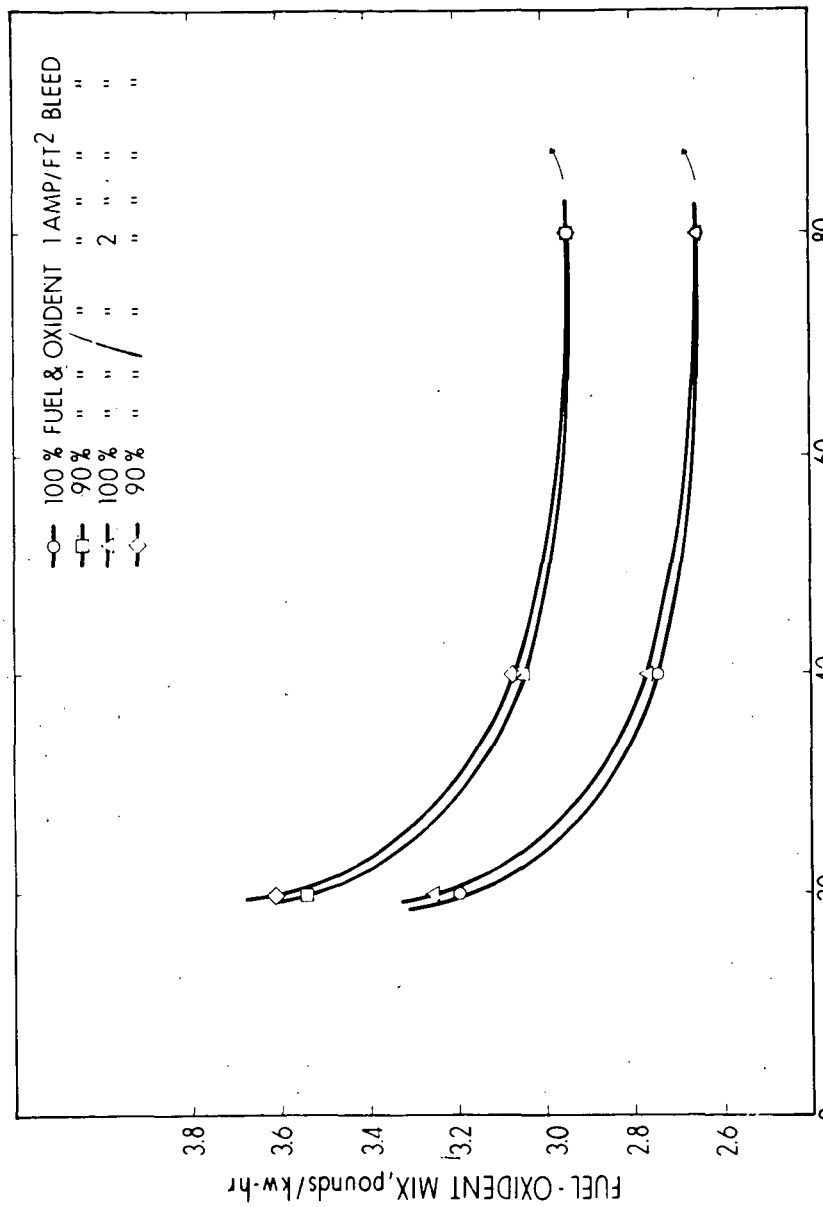

Figure 9 - Effect of loading on the hydrazine-peroxide requirements per kw-hr.

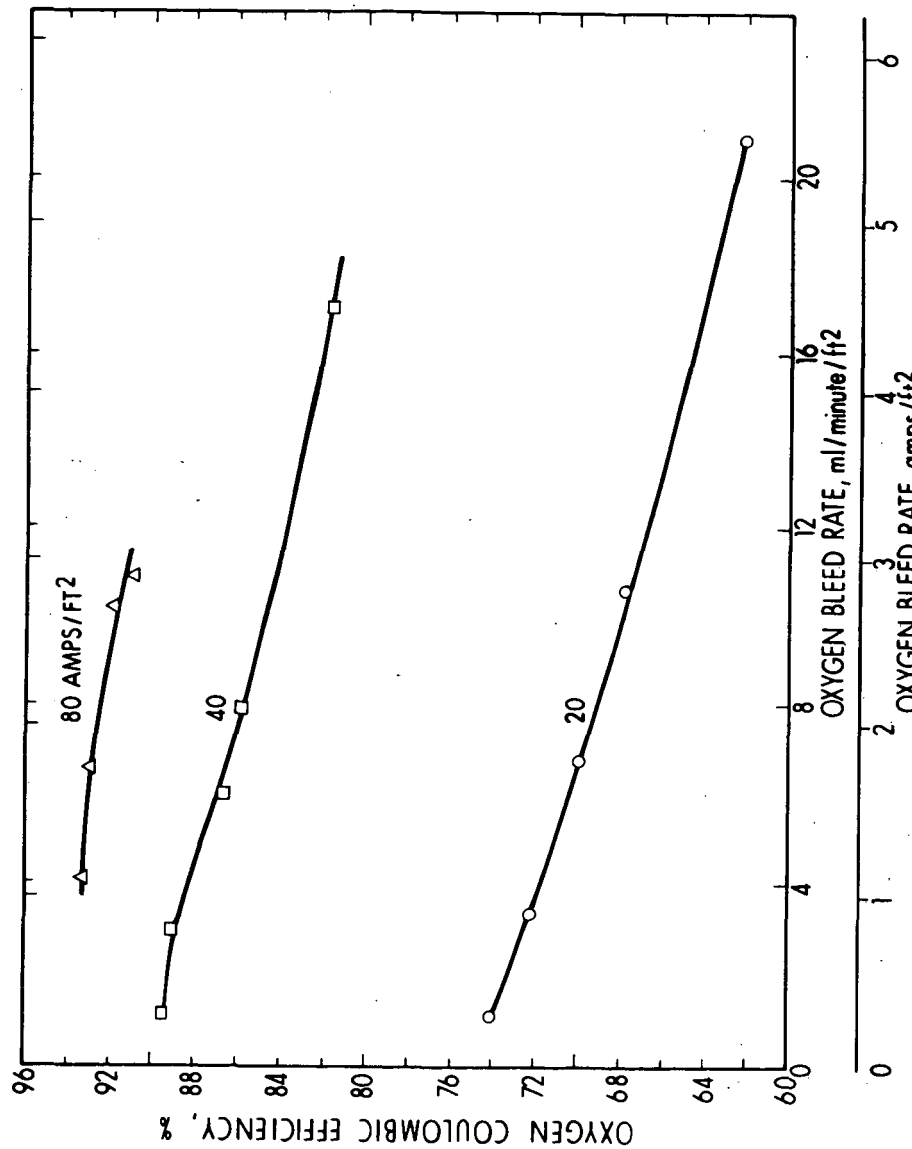

Figure 10 - Effect of oxygen bleed rate on the coulombic efficiency of cathodic oxygen or peroxide consumption.

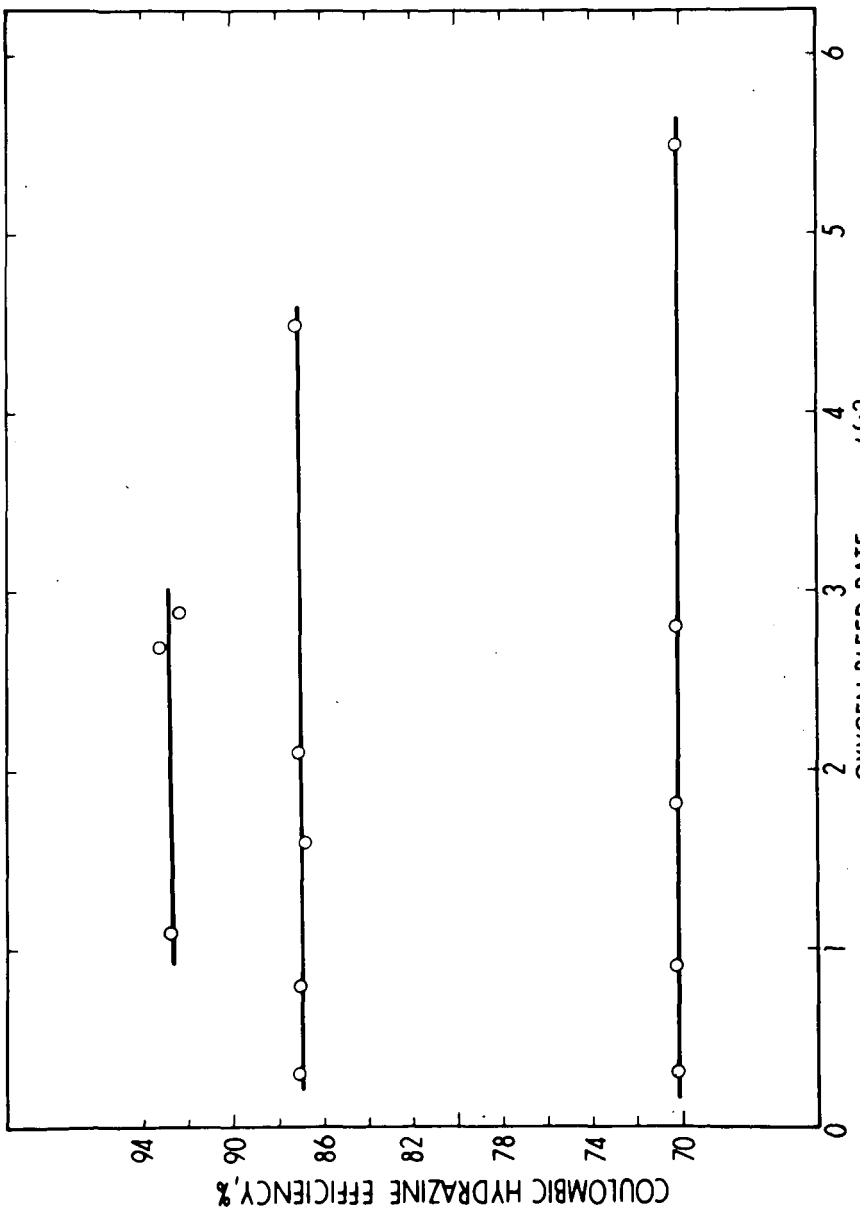

Figure 11 - Effect of oxygen bleed rate on the coulombic efficiency of anodic hydrazine consumption.

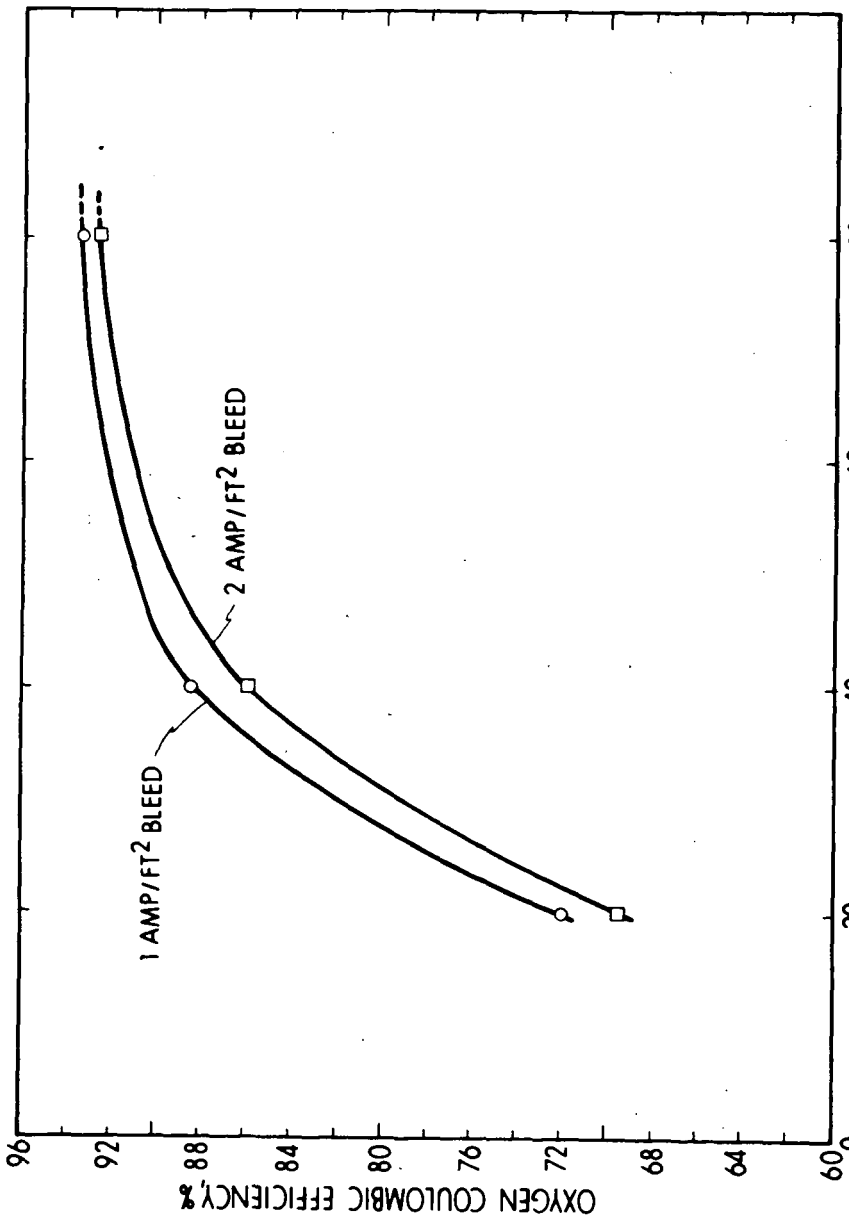

Figure 12 - Effect of loading on the coulombic efficiency of cathodic oxygen or peroxide consumption.

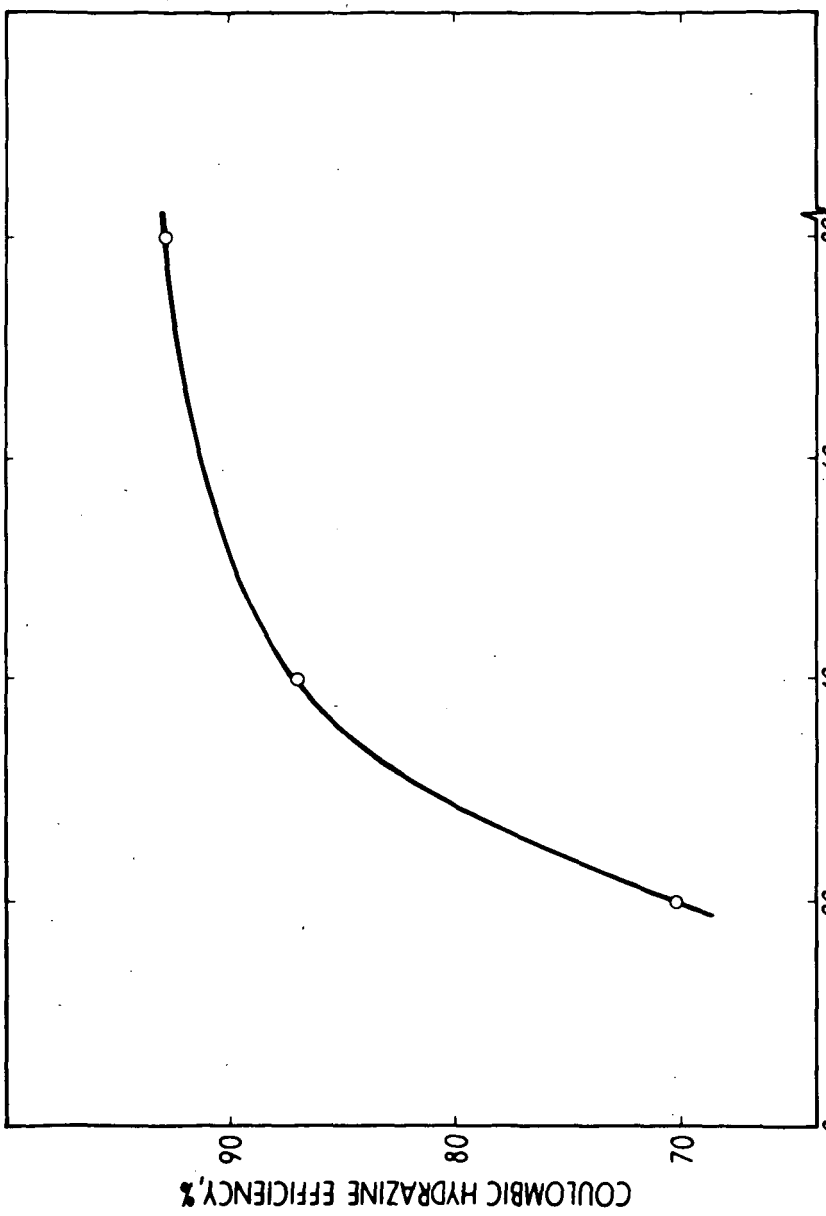

Figure 13 - Effect of loading on the coulombic efficiency of anodic hydrazine consumption.